XI International Conference on Computational Plasticity. Fundamentals and Applications
COMPLAS XI
E. Oñate, D.R.J. Owen, D. Peric and B. Suárez (Eds)

ON THE PREDICTION OF THE CURVATURE OF CROSS ROLL STRAIGHTENED BARS

A. MUTRUX, B. BERISHA AND P. HORA

Institute of Virtual Manufacturing
ETH Zurich
Tannenstr. 3, 8092 Zurich, Switzerland
e-mail: mutrux@ivp.mavt.ethz.ch

Key words: Cross roll straightening, cyclic softening

Abstract. A recently proposed procedure for the simulation of cross roll straightening allows to predict successfully the residual stress distribution in straightened bars as well as their yield stress. Although the procedure allows also to make predictions about the curvature of straightened bars, large discrepancies appear between predictions and experiments. The present study aims at understanding the causes of these deviations. The standard experimental setup for the measurement of curvature provides values on the assumption of a constant in-plane curvature. Using a modified procedure for the prediction of the curvature, this study shows that, according to the model, the curvature of straightened bars is not constant and not in-plane. The reason for the deviation observed between predictions and measurements is then obvious.

1 INTRODUCTION

Cross roll straightening is the last mechanical operation in the production process of bright steel bars and aims principally at reducing: (1) the curvature and (2) the detrimental residual tensile stresses on, and close to, the surface of round bars. On the downside, the operation may lead to a decrease of the yield stress of the bars. Modelling approaches to describe the process can be grouped into two main categories: analytical procedures and FE based procedures. The former ones (see e.g. [1, 2]) relie on the assumption of straightening under pure alternate bending and cannot take into account such influences as the lateral stamping applied by the rolls on the bar. The latter ones (see e.g. [3, 4]) are CPU cost intensive and, therefore, require the use of relatively rough meshes, making them unable to predict subtle differences in e.g. the yield stress of straightened bars.

During cross roll straightening, the bar is bent and stamped between two rotating rolls, a convex and a concave one, as shown in Figure 1. Apart from the geometry of the

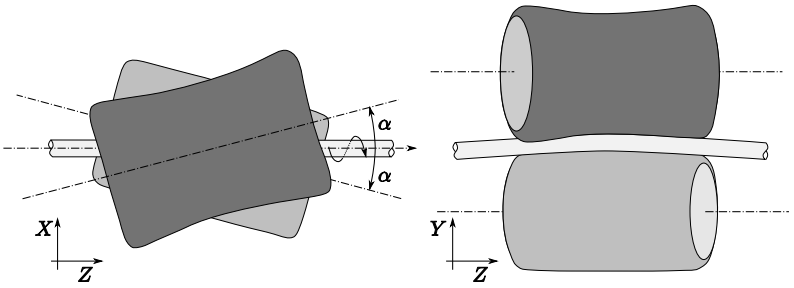

Figure 1: Sketch of the cross roll straightening process. The two main process parameters are the angle α and stamping δ. XYZ are the principal axes of the global coordinate system.

rolls, the main process parameters are the angle α between the rolls and the bar and the stamping δ, defined as the diameter of the bar minus the minimum distance between the rolls. During straightening, the rolls rotate, inducing a forward motion of the bar and a rotation about its main axis.

A mixed analytical-numerical modelling approach to cross roll straightening, based on similar assumptions as the one introduced in [5], is presented in [6]. The procedure allows to predict quantitatively the influence of the straightening parameters α and δ on the yield stress of straightened bars. The predicted residual stress distribution is in qualitative agreement with the measurements presented in [7].

In [6], only intermediate results about the prediction of the curvature of straightened bars are presented. The predictions lie about an order of magnitude higher than the experimental values and no satisfying explanation of this discrepancy is provided. The present study aims at shedding light on the capabilities of the procedure regarding the prediction of the curvature of bars after straightening.

2 PROCESS MODELLING

This section presents a summary of the modelling approach. A more detailed explanation can be found in [6]. The main assumptions on which the procedure rely are the following:

- a *closing* simulation, in which the bar is simply bent and stamped between two static rolls (without rotation or forward feed), provides a decent approximation of the total strain distribution in a bar during cross roll straightening. For example, the influence of the rolling contact between the bar and the rolls can be neglected

- the total strain distribution in the bar depends marginally on the behaviour of the material

- the path of a material point of the bar during straightening can be computed analytically

The first step of the procedure is a *closing* simulation. This simulation is conducted using a dynamic implicit scheme and the material behaviour is described using a linear isotropic model. The results are the total strain distribution within the bar and the bending line $b(t)$. $b(t)$, with $t \in [0,1]$, is a parameterised curve in the ZY plane passing through the nodes lying on the neutral axis of the bar in the deformed configuration. A coordinate system $\{\xi(t), \eta(t), \zeta(t)\}$ is associated to $b(t)$

$$\begin{aligned} e_\xi(t) &= \begin{pmatrix} 1 \\ 0 \\ 0 \end{pmatrix} \\ e_\eta(t) &= \frac{1}{\|b'(t)\|} \begin{pmatrix} 0 \\ b'_z(t) \\ -b'_y(t) \end{pmatrix} \\ e_\zeta(t) &= \frac{1}{\|b'(t)\|} \begin{pmatrix} 0 \\ b'_y(t) \\ b'_z(t) \end{pmatrix} \end{aligned} \tag{1}$$

where $b'(t)$ is the directional derivative of $b(t)$.

A sufficient number of points P_i are chosen over a cross section of the bar. Their helical paths $p_i(t)$, having $b(t)$ as neutral axis and a pitch $\varkappa = 2\pi r_{rod} \tan(\alpha)$, are computed. The solids lying on each path are identified. The sequence of the total strain tensors associated to these elements builds the total strain history of each material point considered. Total strain increments are defined as the differences between consecutive states along a given path. Those strain increments are then integrated according to the constitutive equations presented in Section 3.2. To compensate for eventual deviations from the state of equilibrium, the internal variables obtained for each P_i are mapped to a corresponding layer of solid elements and, applying adequate boundary conditions, the equilibrium is sought using a one-step static implicit solution scheme.

For predictions regarding the evolution of the curvature of the bar, axis asymmetric axial initial stresses are considered. An initial curvature $\kappa^{bs} < \sigma_y / (E r_{rod})$ of a bar can be reduced to a stress distribution over its cross section according to relation

$$\sigma^{in}_{\zeta\zeta}(\eta) = E\kappa^{bs}\eta \tag{2}$$

Considering $\sigma^{in}_{\zeta\zeta}$ as initial stresses, the corresponding $\sigma^{out}_{\zeta\zeta}$ stresses after straightening are computed using the procedure described above. This stress distribution generates a moment $M_{\tilde{\xi}}$ about an axis $\tilde{\xi}$

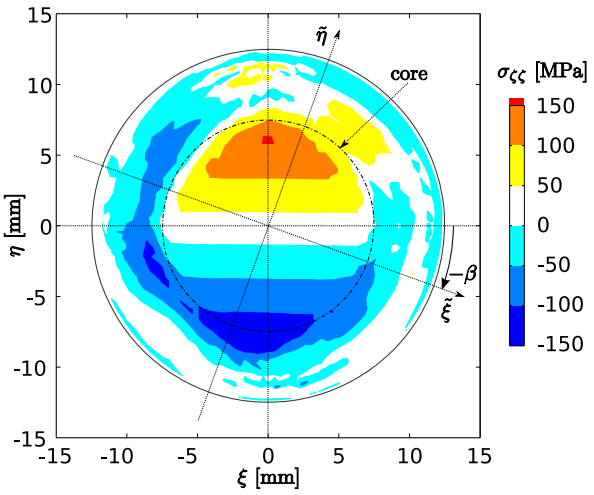

Figure 2: $\sigma_{\zeta\zeta}^{out}$ stress distribution in a bar with an initial curvature $\kappa^{bs} = 10^{-4}$ straightened with $\alpha = 18°$ and $\delta = 0.50$ mm. The angle β is highlighted ($\beta = -20°$ in the present case). The linear initial stress distribution in the core of the bar is not affected by the plastification that takes place in the peripheral layers.

$$M_{\tilde{\xi}} = \int_A \sigma_{\zeta\zeta}^{out} \tilde{\eta} dA \tag{3}$$

where $\tilde{\xi}\tilde{\eta}$ is obtained by a rotation of $\xi\eta$ by an angle β around the axis ζ, as shown in Figure 2. The moment $M_{\tilde{\xi}}^{max}$ is

$$M_{\tilde{\xi}}^{max} = \max\left(M_{\tilde{\xi}}\left(\beta\right)\right) \tag{4}$$

The curvature after straightening is $\kappa^{as} = M_{\tilde{\xi}}^{max} / \left(EI\right)$.

3 MATERIAL MODELLING

3.1 Tension-compression tests

The material investigated in the context of this study is a SAE 1144 medium carbon steel ($\varnothing$25 mm). As mentionned above, cross roll straightening induces a cyclic deformation in the bar. The cyclic behaviour of the material is investigated by carrying out tension-compression tests under total strain control with an amplitude $\Delta\varepsilon/2 = 1.5{\cdot}10^{-2}$ at a strain rate of approximately $5 \cdot 10^{-3}$ 1/s. The material exhibits a strong Bauschinger effect, cyclic softening and a small apparent tension-compression asymmetry. The term *apparent* is used to highlight the fact that the phenomenon is more likely due to a Bauschinger effect from the previous drawing operation than to a *real* (according to the definition given in [8]) strength differential effect.

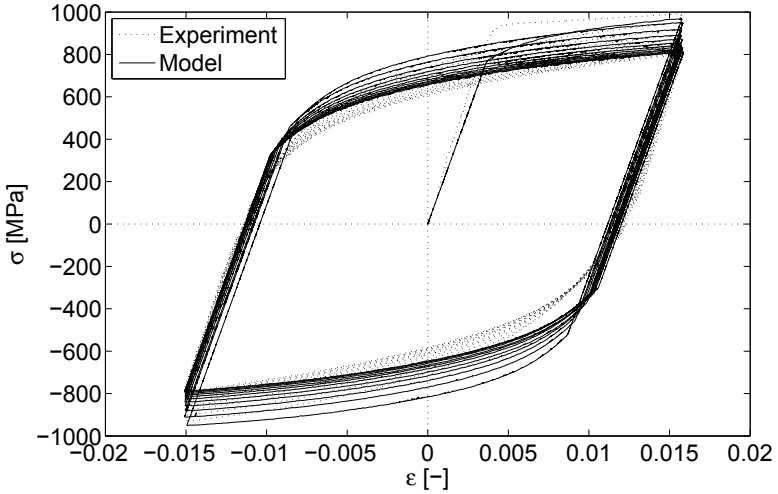

Figure 3: Stress-strain curve obtained from a tension-compression test and corresponding values according to the Chaboche model.

3.2 Constitutive equations

The total strain tensor is additively decomposed in an elastic strain and a plastic strain. The elastic part of the strain tensor obeys Hooke's law. The plastic strain components are governed by the associated flow rule. The yield function is expressed as

$$F = \frac{3}{2}(\boldsymbol{s} - \boldsymbol{a}) : (\boldsymbol{s} - \boldsymbol{a}) - Y^2 \tag{5}$$

where $\boldsymbol{s}$ is the deviatoric stress tensor and $\boldsymbol{a}$ is the backstress tensor. Y, the isotropic hardening (or softening) part, is

$$Y = Q(1 - \exp(-bp)) + \sigma_0 \tag{6}$$

where p is the accumulated plastic strain. $\boldsymbol{a}$ (i.e. its evolution equation) is decomposed according to [9] as

$$\boldsymbol{a} = \sum_{i=1}^{M} \boldsymbol{a}^{(i)} + \boldsymbol{a}_0 \tag{7}$$

where $\boldsymbol{a}_0$ allows to take into account the initial asymmetry between tension and compression in a non-evanescent manner. $\boldsymbol{a}^{(i)}$ is defined through the (Armstrong-Frederick) differential equation

$$\mathrm{d}\boldsymbol{a}^{(i)} = \frac{2}{3} C_i \mathrm{d}\boldsymbol{\varepsilon}^p - \gamma_i \boldsymbol{a}^{(i)} \mathrm{d}p \tag{8}$$

Figure 3 shows the fitted model on the experimental stress-strain curve; the corresponding values of the parameters are given in Table 1. The material model is implemented according to the radial return algorithm presented in [10]. For the *closing* simulation mentionned in Section 2, a linear isotropic model is fitted on the first tension branch ($\sigma_y = 935$ MPa and $E_{tan} = 3000$ MPa).

Table 1: Fitted parameters for the Chaboche model ($E = 210$ GPa and $M = 3$)

C_1	C_2	C_3	γ_1	γ_2	γ_3	Q	b	σ_0	$\boldsymbol{a}_{33}$
44400	18100	1430	665	87	0	-214	5.5	757	7.7

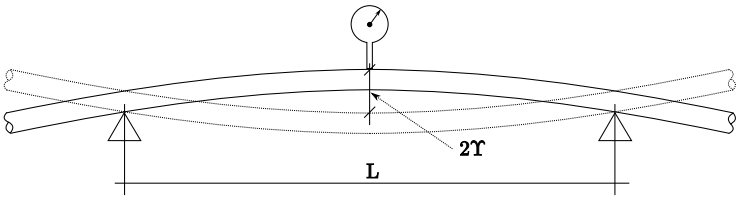

Figure 4: Experimental setup used to measure the curvature of bars ($L = 1$ m).

4 PREDICTION OF RESULTING STRAIGHTNESS

The curvatures of 40 bars before and after straightening with $\alpha = 18°$ and $\delta = 0.50$ mm are measured using the setup sketched in Figure 4. The setup is a common means of assessing the curvature of bars in the industry and [11] presents measurements obtained using a similar device, the dial gauge being replaced by a laser one. The maximum dial gauge amplitude 2Υ is recorded and is converted into a curvature $\kappa = 8\Upsilon/L^2$ assuming that the bar has a constant radius of curvature in a single plane. Experimental results and corresponding predictions are plotted in Figure 5.

It appears from Figure 5 that the curvatures predicted by the model are about an order of magnitude higher than the experimental values. A straightening effect can be predicted when relatively large values of curvature before straightening are considered. When bars with a small initial curvature are considered, such as the ones investigated in this study, the predicted curvatures after straightening are larger than the ones before straightening.

In [11], the roller leveller straightening of coiled medium carbon steel wire (⌀6 mm) is investigated both experimentally and numerically. In a roller leveller, the bar is repeatedly bent in a single plane. Considering a bar initially curved in a single plane and straightening it in its plane of curvature leads to (1) a reduction of its main curvature and (2) the appearance of a small out-of-plane curvature. In this case, the assumption that straightened bars are curved in a single plane does not hold.

In order to verify the hypothesis of the constant in-plane curvature of the bars after straightening for the present case, κ^{as} is computed for different sections over a distance $\varkappa$ of the bar ($\varkappa = 25.52$ mm for $r_{rod} = 12.5$ mm and $\alpha = 18°$). The computations are made with $\alpha = 18°$ and $\delta = 0.50$ mm and two initial curvatures are considered: (1) $\kappa^{bs} = 0$ and

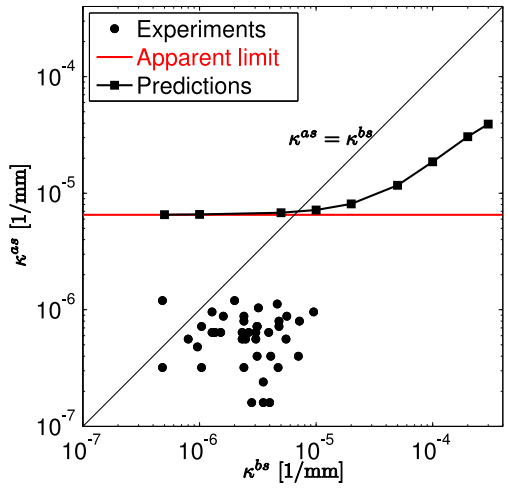

Figure 5: The curvatures before (κ^{bs}) and after (κ^{as}) straightening (with $\alpha = 18°$ and $\delta = 0.50$ mm) of 40 bars are measured. The values predicted by the model are also plotted. The model cannot, apparently, predict curvatures below $\kappa^{as} = 6.5 \cdot 10^{-6}$ 1/mm.

(2) $\kappa^{bs} = 10^{-4}$ 1/mm. The predicted curvatures as well as the corresponding angles β are plotted in Figure 6.

It appears from the results obtained for $\kappa^{bs} = 0$ (Figure 6 (top)) that:

- the curvature of the bar after straightening is approximately constant ($\kappa^{as} \approx 6.6 \cdot 10^{-6}$ 1/mm, which corresponds to the *apparent limit* highlighted in Figure 5)
- the angle β between the axis of principal curvature and the axis ζ completes a whole rotation over a distance $\varkappa$

According to the model, the shape after straightening of an initially perfectly straight bar is hence a helix whose main axis is a straight line. Random numerical errors lead to variations $2\Delta\kappa^{as} < 5 \cdot 10^{-7}$ 1/mm, which are acceptable considering the scattering of the experimental data.

It appears from the results obtained for $\kappa^{bs} = 10^{-4}$ 1/mm (Figure 6 (bottom)) that:

- the curvature of the bar after straightening varies over a length $\varkappa$
- the angle β varies in a $\pm 30°$ strip

These results highlight the fact that the comparison made in Figure 5 between experimental (global) values of curvature and predicted (local) curvatures is not relevant. The assumption of a constant in-plane curvature after straightening does not hold. The experimental setup pictured in Figure 4 is not sufficient to assess the curvature of straightened bars.

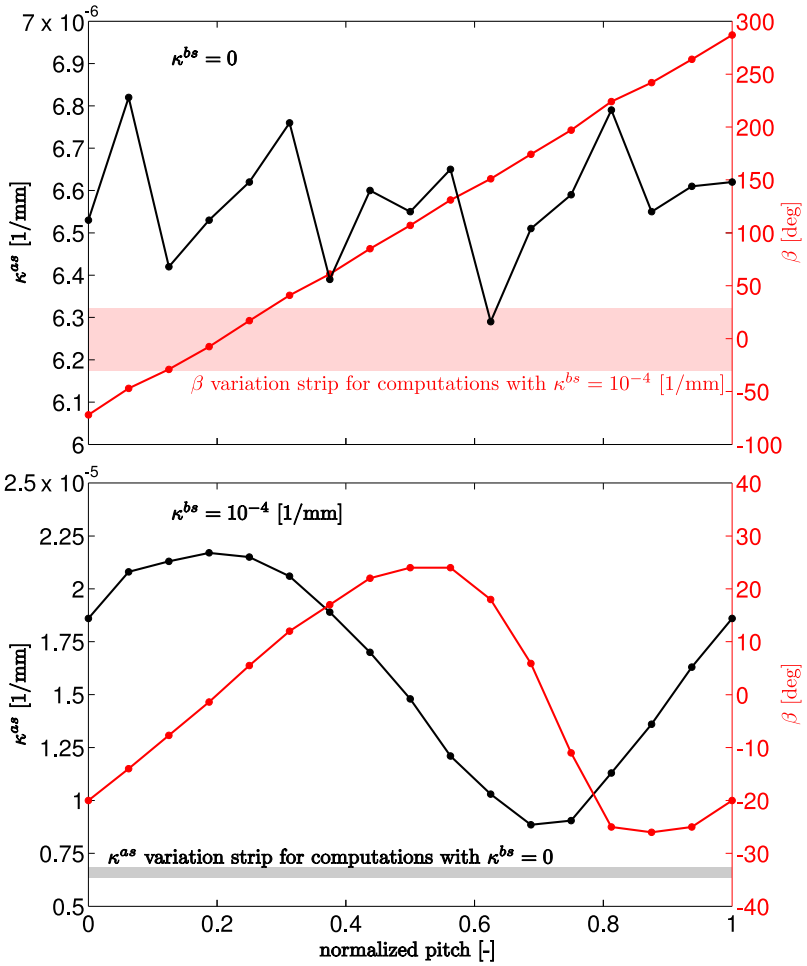

Figure 6: Predicted curvatures after straightening (κ^{as}) and the corresponding angles to the axis ξ for two different curvatures before straightening: $\kappa^{bs} = 0$ (top) and $\kappa = 10^{-4}$ 1/mm (bottom).

5 CONCLUSIONS

The present study sheds light on the causes of the large discrepancy observed between measurements and experiments in [6]. Using a standard experimental setup, the curvature of bars is measured on the assumption of a constant in-plane curvature. Although drawn bars may exhibit such curvatures, it is shown numerically that the assumption does not hold for straightened bars. A meaningful link, if any, between predicted (local) and measured (global) values is still to be established.

REFERENCES

[1] Das Talukder, N.K. and Johnson, W. On the arrangement of rolls in cross-roll straighteners. *Int. J. Mech. Sci.* (1981) **23**:213–220.

[2] Wu, B.J., Chan, L.C., Lee, L.C and Ao, L.W. A study on the precision modeling of the bars produced in two cross-roll straightening. *J. Mater. Proc. Technol.* (2000) **99**:202–206.

[3] Mutrux, A., Berisha, B., Hochholdinger, B. and Hora, P. Numerical modelling of cross roll straightening. *Proc. 7th LS-Dyna Anwederforum* (2008).

[4] Kuboki, K., Huang, H., Murata, M., Yamaguchi, Y. and Kuroda, K. FEM analysis of tube straightener adopting implicit scheme. *Steel Res. Int.* (2010) **9**:584–587.

[5] Furugen, M. and Hayashi, C. Theory of tube deformation on cross roll straightening. *Proc. 3rd Int. Conf. Steel Rolling* (1985) 717–724.

[6] Mutrux, A., Berisha, B., Hora, P. Prediction of cyclic softening in a medium carbon steel during cross roll straightening. *J. Mater. Proc. Technol.* (2011) DOI 10.1016/j.jmatprotec.2011.03.019.

[7] Davis, J.R. and Mills, K.M (eds.). *Metals Handbook, vol. 1: Properties and Selection: Irons, Steels, and High-Performance Alloys*. ASM International, p. 258, (1990).

[8] Banabic, B. (ed.) *Advanced Methods in Material Forming*. Springer, p. 3, (2007).

[9] Chaboche, J.L. Time-independent constitutive theories for cyclic plasticity. *Int. J. Plast.* (1986) **2**:149–188.

[10] Kobayashi, M. and Ohno, N. Implementation of cyclic plasticity models based on a general form of kinematic hardening. *Int. J. Num. Methods Engng.* (2002) **53**:2217–2238.

[11] Asakawa, M., Urabe, M., Nishimura, K., Hamada, R., Aizawa, S. and Amari, M. Theoretical and experimental analysis of roller leveller straightening for coiled bar. *Steel Res. Int.* (2010) **81(9)**:242–245.